Synthesis of Antimony Oxide Nano-particles by Thermal Oxidation

C. H. Xu, S. Q. Shi* and Q. Tang

Department of Mechanical Engineering, The Hong Kong Polytechnic University,
Hung Hom, Kowloon, Hong Kong, China, *mmsqshi@polyu.edu.hk

ABSTRACT

Sb_2O_3 nano-particles are synthesized by thermal oxidation in this research. Pure Sb granular is put in the middle of a tube furnace at an air pressure of 1 atm with a flow rate of 4.0 ml/min. The furnace temperature at the position of samples is set at 550°C. Si wafer, glass and Al foil are used as substrates, which are put the downstream of gas flow to collect Sb oxide. The collected Sb oxides on different substrates are examined with field emission scanning electron microscopy, X-ray diffractometer and transmission electron microscopy. Sb oxide obtained in this method shows Sb_2O_3 nano-particles with strong {111} growth texture. The mechanism of synthesis of Sb_2O_3 nano-particles is analyzed, based on the experiment results.

Keywords: anitomony oxide, nano-particles, thermal oxidation, field emission scanning electronic microscope, X-ray diffraction.

1 INTRODUCTION

Antimony (Sb) oxide can be used as catalyst, retardant, fining agent and optical materials [1]. Recently, hydrous Sb oxide was found to have high proton conductivity, which is likely to be a promising humidity-sensing materials [2, 3]. Sb_2O_3 plus ZnO have been used to make films that can be used as gas sensor materials [4].

Nano-particles have increasingly attracted interest over the past decade due to the possibilities of novel or even outstanding properties compared with bulk materials. Semiconductor nanocrystaline materials have been an area of intense investigation [5, 6]. It was reported recently that the synthesis of Sb oxide nano-particles can be done by the chemical method [7] and γ-ray radiation-oxidation route [8], in which $SbCl_3$ and NaOH are used as starting materials. Another reported method of synthesis of Sb oxide nano-particales is vapor condensation, which includes three steps: melting Sb by laser, oxidizing vapor Sb and condensing Sb oxide [9]. However, the mixture of Sb and Sb oxide nano-particles is usually obtained in this method. The experiment equipment is also expensive.

In this paper we report the synthesis of antimony oxide nano-particles by heating metal Sb in solid state in oxidative environment and collecting vapor Sb oxides on the substrates of Si wafer, Al foils, and glass at the downstream of gas flow.

2 EXPERIMENT PROCEDURE

Commercial antimony (Sb) granular with average diameter of 1.5 mm (purity: 99.99% Sb) is used in the present experiment. Sb granulars on an alumina crucible are put in the middle of a tube furnace in compressed air at a pressure of 1 atm with a constant flow rate of 4.0 ml/min for 4 hours. The furnace temperature at the position of samples is set at 550°C. Si (001) wafer, glass and Al foil are used as substrate materials and the substrates are put the downstream of gas flow to collect Sb oxide.

After oxidation, the as-synthesized Sb oxides on the substrates show a white color. The crystal structures of the collected Sb oxides on the substrates are directly examined with a Philips PW3710 X-ray diffractometer, using a 40 kV, 30 mA, Cu Kα X-ray. Morphologies of the collected Sb oxide on the substrates are also characterized by a field emission scanning electron microscopy (JEOL JSM-6335F). The collected Sb oxides on the substrates are dispersed into ethanol. The bottle of the ethanol solution is put in an ultrasonic machine (COLE-Parmer 8890) for 10 min to separate Sb oxides from the substrates. Then the resulting solution is dropped onto a carbon coated TEM copper grid. Transmission electron microscopy (TEM) imaging, electron diffraction and local composition analysis are performed on the samples on the TEM grid using a JEOL 2010F TEM with an energy dispersive (X-ray) spectroscopy (EDS) system, operated at 200 kV.

3 EXPERIMENT RESULTS

3.1 Shape and Size of Nano-particles

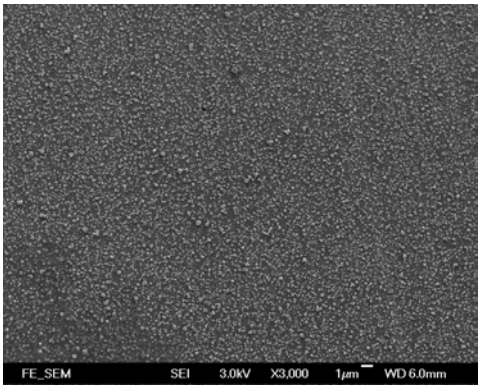

(a)

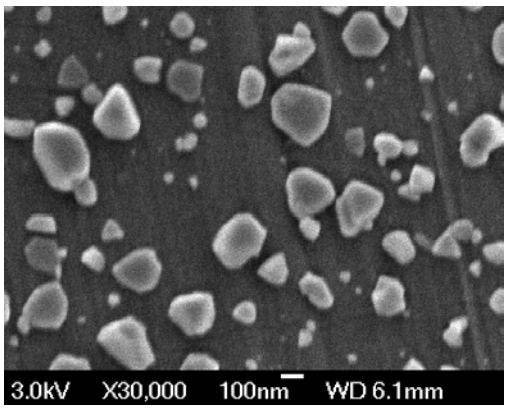

(b)

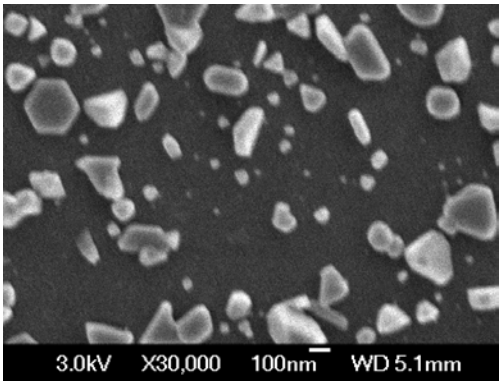

(c)

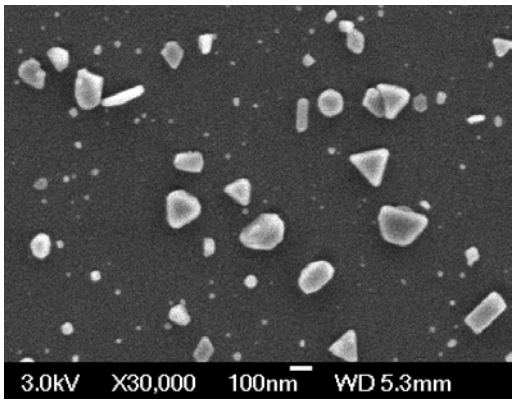

(d)

Figure 1 Morphologies of the collected Sb oxides on the substrate of: (a) Al foil at low magnification, showing uniform particles, (b) Al foil (c) glass and (d) Si (001) wafer at high magnification

The Sb oxide nano-particles uniformly distribute on the substrates. Fig. 1(a) shows the uniform Sb oxide particles on the substrate of Al foil. The shapes and sizes of the collected nano-particles can be seen clearly at high magnifications. Fig 1(b), (c), (d) are the morphologies of the nano-particles on the substrates of Al foil, glass, and Si (001) wafer at high magnifications, respectively. The nano-particles on the different substrate have similar features. The sizes of the nanoparticles are at the range of 10 ~ 200 nm. Large particles show significant crystalline structures. The shapes of these particles include triangle, hexagon, rectangular.

3.2 X-Ray Diffraction

The X-ray diffraction results show that the phase of the collected Sb oxide is Sb_2O_3 with face-centered cubic structure. Only (111), (222) and (444) diffraction peaks occur on XRD spectra, suggesting a strong growth textures of Sb_2O_3 on all three type of substrates. X-ray spectrum of the collected nano-particles on the substrate of glass is shown in Fig. 2(b). An X-ray spectrum for the Sb specimen before oxidation is shown in Fig 2(a). Comparing the two spectra, it can be concluded that no metal Sb is in the collected particles.

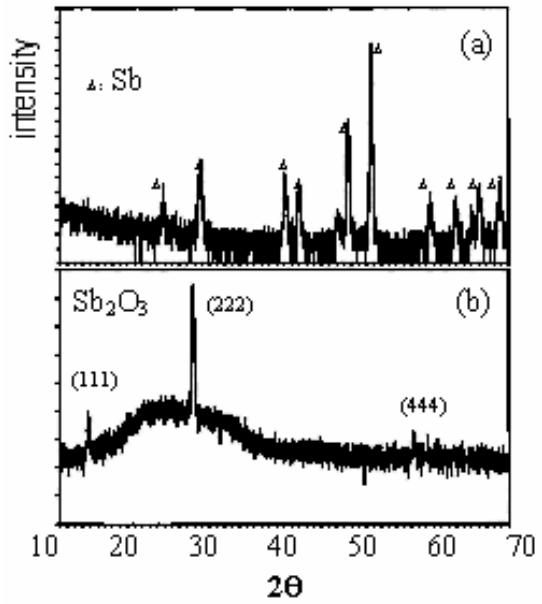

Fig. 2 X-ray spectra (a) pure metal Sb before oxidation and (b) the collected Sb_2O_3 oxides on the glass substrate, showing strong growth texture of (111).

3.3 TEM Results

TEM images in Fig. 3 show Sb oxide nano-particles. Fig. 3(a) shows the morphologies of Sb oxides. The grain size changes from 10 to 150 nm. A large grain tends to be in triangle shape in Fig. 3(a). The corresponding selected area electron diffraction pattern of the triangle grain is illustrated at the right bottom corner. The pattern comes form {440} of Sb_2O_3, which indicates the surface of the triangle Sb oxide is (111) of Sb_2O_3. Fig. 3(b) is a high resolution image taken on the triangle Sb_2O_3 grain in Fig. 3(a). The space of 1.95 A is corresponding for the (440) plane of Sb_2O_3. The Fig. 3(c) is the EDS result of nano-particles in Fig. 3(a), showing Sb and O elements (Cu and C in Fig. 3(c) come from a carbon coated TEM copper

grid).

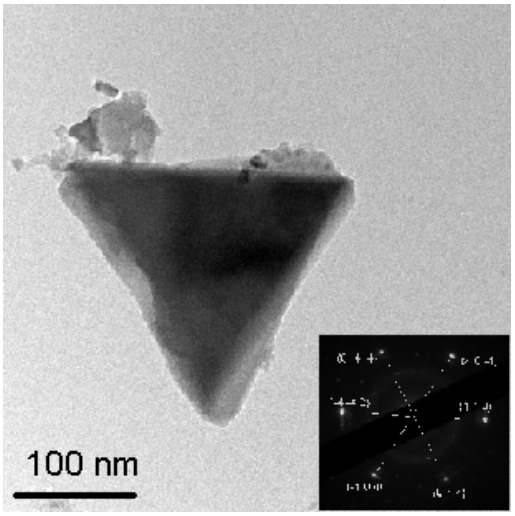

(a)

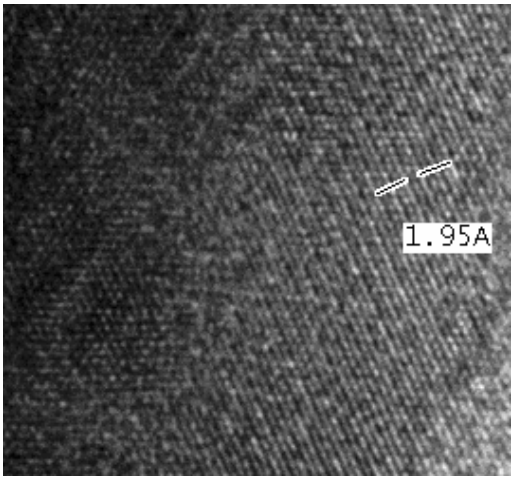

(b)

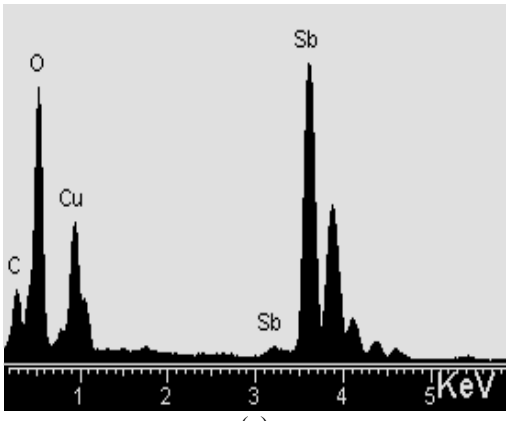

(c)

Fig. 3 TEM images for Sb_2O_3 oxide particles (a) morphology and corresponding selected area electron diffraction of a large triangle grain and (b) a high resolution image taken from the triangle Sb_2O_3, and (c) the EDS result of nano-particles, showing Sb and O

4 DISCUSSIONS

4.1 Phase of Collected Nano-particles

After the oxidation of pure metal Sb in air at 550°C, the collected oxides on the substrates of Si wafer, Al foils and glass at the positions of the downstream of gas flow are Sb_2O_3 with strong {111} growth textures. The size of the nano-oxide particles is in the range of 10 ~ 200 nm. It was reported that melting metal Sb in oxidation environment by laser can be used in syntheses of Sb_2O_3 nano-particales. This technique includes three steps: melting Sb by laser, oxidizing vapor Sb and condensing Sb oxide [9]. The mixture of Sb and Sb oxide nano-particles is usually obtained in this method, due to melting metal during the process. In present experiment, pure Sb_2O_3 nano-oxide is obtained from X-ray spectra in Fig. 2(b). The furnace temperature at the position of Sb metal is set at 550°C, which is less than the melt point of Sb (630°C). According to Sb-O phase diagram [10], the high oxygen phase of Sb_2O_5 can be formed at high oxygen partial pressure, such as in air. The solid Sb_2O_5 oxide decomposes into liquid SbO_2 and O_2 at 525 °C under 1 atm. Compared with metal Sb, Sb oxide moves easily with gas flow, and the temperature of oxidation is higher than the decomposition temperature of Sb_2O_5 oxide. However, the collected oxide on the substrates in the experiment is Sb_2O_3 (not SbO_2). In order to explain the reason, more experiments are needed. We will analyze this in another report in details.

4.2 Growth Texture of Sb_2O_3 Oxide

It can be concluded based on the analysis on X-ray spectra in Fig. 2 that the collected white oxide on the substrates are face-centered cubic Sb_2O_3 with extensive strong {111} growth texture. It can be seen from Fig. 2 that three types of the substrate do not affect the formation of Sb_2O_3 nano-particles much, which can be understood from the crystalline structures of oxide and substrates. The structure of glass substrate is amorphous. The average atomic distance of the glass ($d_{average}$) can be evaluated from the X-ray diffraction pattern in Fig. 2(b). There is widen peak at the position of $2\theta = 15 - 35°$ on the background curve, which stands for the average atomic distance of amorphous material, glass. This distance of $d_{average}$ can be calculated by follow equation [14]

$$d_{average} = \frac{\lambda}{2\sin(\theta)} \qquad (1)$$

where λ is the wavelength of diffraction beam, Cu kλ (=1.541 A). The calculation results are listed in Table 1. When one type of material is deposited on a substrate, there are three types of interfaces between a deposition and a substrate, namely coherent, semicoherent and incoherent

[11, 12, 13], depending on the crystalline parameters of the deposition and the substrate. Lattice parameters of Sb_2O_3 and substrates of Al, Si, and glass show big different, as shown in Table 1, so it is easy to form incoherent interface between Sb_2O_3 oxide and the substrates. For this reason, the morphologies of Sb_2O_3 oxides formed on the different substrate are similar.

phase	structure	lattice parameter (A)	Ref.
Sb_2O_3	FCC	a = 11.152	[14]
Al	FCC	a = 4.049	[14]
Si	Diamond cubic	a = 5.428	[14]
Glass	Amorphous	$d_{average}$ = 5.902 – 2.562	

Table 1: Crystalline structures and parameters of materials

The planar energy in a crystal reverses its inter-planar distance *d*. In other word, the plan with the highest density has the lowest energy. {111} planes in face-centered cubic have the highest density [15]. The crystalline structure of Sb_2O_3 oxide is face-centered cubic. In order to remain the lowest energy in the system, the {111} planes dominate on the surface so that the {111} texture Sb_2O_3 oxide forms on different substrates. Recently, three-dimensional molecular dynamics simulation has also indicated that {111} planes in face-centered cubic have the lowest energy [16].

The grains of the collected Sb_2O_3 oxide are in the range of 10 ~ 200 nm, as shown in Fig. 1 and Fig. 3. The large grains show significant crystalline structures, including triangle, hexagon, and rectangular, while small ones tend to be in round shape. When a new phase forms, the formation energy of the new phase includes surface energy and misfit strain energy. The shape of a new phase is determined by maintaining the lowest energy state in the system. For an incoherent Sb_2O_3-substrate interface, the system energy is dominated by the surface energy because the misfit strain energy is small. In order to achieve the lowest surface energy, the new phase with a small size appears round shape. When the grains of new phase grow larger, the energy difference on various planes becomes significant. The surface of new grains contacted with air is dominated by {111} planes of Sb_2O_3 in order to reduce the total surface energy. Therefore, the large grains show crystalline structures, such as triangle, hexagon and rectangular shapes.

5 CONCLUSIONS

The following conclusions can be drawn:

1. Pure Sb_2O_3 nano-particle oxides can be synthesized by heating metal Sb at 550°C under a pressure of 1 atm in a constant air flow rate and collecting vapor oxides on a substrate at the downstream of gas flow.

2. The size of the Sb_2O_3 nano-particle oxides is in the range of 10 ~ 200 nm.

3. Sb_2O_3 oxides show the strong {111} growth texture, which is independent on the substrates of Al, Si and glass.

ACKNOWLDGEMENTS

This work was funded by Research Grant Council of Hong Kong (B-Q747).

REFERENCES

[1] G. V. Samsonov, "The Oxide Handbook", IFI/Plenum, 320-441,1973

[2] K. Ozawa, Y. Sakka and A. Amamo, Journal of Materials Research, 13, 830, 1998

[3] D. J. Dzimitrowice, J. B. Goodenough and P. J. Wiseman, Mater. Res. Bull. 17, 971, 1982

[4] B. L. Zhu, C. S. Xie, A. H. Wang, D. W. Zheng, M. L. Hu and W. Y. Wang, Materials Research Bulletin, 39, 409-415, 2004

[5] W. Q. Han, S. S. Fan, Q. Q. Li and Y. D. Hu, Science, 277, 1287, 1997

[6] A. M. Morales and C. M. Liber, Science 279, 208, 1998

[7] Z. L. Zhang, L. Guo, and W. D. Wang, Journal Of Materials Research 16, 803-805, 2001

[8] Y. P. Liu, Y. H. Zhang, M. W. Zhang, W. H. Zhang, Y. T. Qian, L. Yang, C. S. Wang, Z. W. Chen, Materials Science and Engineering B 49, 42-45, 1997

[9] D. W. Zeng, B. L. Zhu, C. S. Xie, W. L. Song and A. H. Wang, Materials science and Engineering A 366, 332-337, 2004

[10] Thaddeus B. Massalski ; editors, Hiroaki Okamoto, P.R. Subramanian, Linda Kacprzak. "Binary alloy phase diagrams", Materilas Park: ASM International, 2912-2913, 1990

[11] J. Mayer, C. P. Flynn, M. Ruhle, Ultramicroscopy, 33, 51, 1990

[12] G. Gutekunst, J. Mayer and M. Ruhle, Philos. Mag. A, 75, 1357, 1997

[13] V. Vitek, G. Gutekunst, J. Mayer, M. Ruhle, Philos. Mag. A, 71, 1219, 1995

[14] D. C. Cullity, "Elements of X-ray Diffraction" Addison-Wesley Publishing Company Inc., 482-485, 1967

[15] Lawrence H. Van Vlack, "Elements of Materials Science and Engineering" Fifth Edition, Addison-Wesley Publishing Company, 63-103, 1985

[16] W. C. Liu, Y. X. Wang, C. H. Woo, and H. C. Huang, Mat. Res. Soc. Symp. Proc. 677, AA7.32.1- AA7.32.5, 2001